https://grupo.us.es/grupotep130/es/

Design optimisation of perforated solar façades in order to balance daylighting with thermal performance

Doris A. Chi, David Moreno, and Jaime Navarro

This is an Accepted Manuscript of an article published by Elsevier: Building and Environment, Volume 125, 2017, Pages 383-400
ISSN 03060-1323

http://dx.doi.org/10.1016/j.buildenv.2017.09.007

CC BY NC SA

Authors' names and affiliations:

Doris A. Chi, David Moreno, and Jaime Navarro
Instituto Universitario de Arquitectura y Ciencias de la Construcción, Universidad de Sevilla, Spain

Corresponding author:

Doris A. Chi, Instituto Universitario de Arquitectura y Ciencias de la Construcción, Universidad de Sevilla, Spain
Email: abigailchi@gmail.com

Abstract

On fully-glazed building façades perforated solar screens (PSS) are often used as an outer skin in order to reduce energy consumption and to solve issues such as visual appearance. However, not only must PSS control solar radiation but they must also provide adequate daylight levels, thus requiring a balanced solution. Currently, daylighting simulation software enables us to perform efficient daylight analysis of spaces with PSS. Notwithstanding this, current energy simulation software such as EnergyPlus cannot deal well with such geometry directly, making the thermal evaluation of PSS an infeasible task. This paper presents a methodology for achieving an integrated analysis of daylighting and energy consumption of spaces with PSS during the design stage. Such methodology provides daylight analysis through DIVA, and thermal analysis through EnergyPlus via DIVA/Grasshopper/Archsim. The aim is to optimise the dual performance of a balanced PSS solution through controlling its perforation percentage, matrix and shape, by using the orthogonal arrays (DOA) statistical method. DOA method is efficient in reducing the number of simulations derived from the combination of the aforementioned variables, and in identifying the optimal PSS configuration. In comparison to a non-optimised façade located in Seville, Spain, the predicted optimal PSS achieved a 50% increase in the actual daylit area and a 55% reduction in the total energy demand.

Keywords: daylight availability; energy consumption; optimal design; orthogonal arrays; perforated solar screens; simulation tools.

1. Introduction

The building envelope plays an important role in controlling and/or admitting the various elements of the external environment. The building envelope can achieve about 80% of an environmental solution, creating an efficient building that interacts with its surrounding environment [1]. Present concerns with energy conservation have induced extensive studies regarding the façade's performance with the environment. There are numerous examples of buildings which have ignored their climatic conditions by extending the use of highly glazed façades in order for them to be airy, light and transparent. However, as there is a risk of high energy demand in order to maintain indoor thermal comfort [2] their energy efficiency has come into question.

Solar shading has, therefore, been an important step in energy saving control for buildings. Shading affects the energy use for lighting, heating and cooling; it also reduces yearly solar gains

originating from solar radiation, as well as modifying thermal exchanges through the glazed building envelope and, moreover, it influences daylight levels within a building [3]. Perforated solar screens (PSS) are a type of shading device that have gained popularity with the shift from traditional to modern architectural styles [4,5]. Generally, PSS are flat, opaque, perforated panels forming a double skin for fully-glazed building façades. The organisation of their perforations filters out direct incident sunlight, which is prevented from directly penetrating into spaces while still allowing users to view the exterior. The opaque parts of the screen reflect sunlight and act as solar control systems [6,7]. For example, Figure 1 illustrates a façade with a PSS.

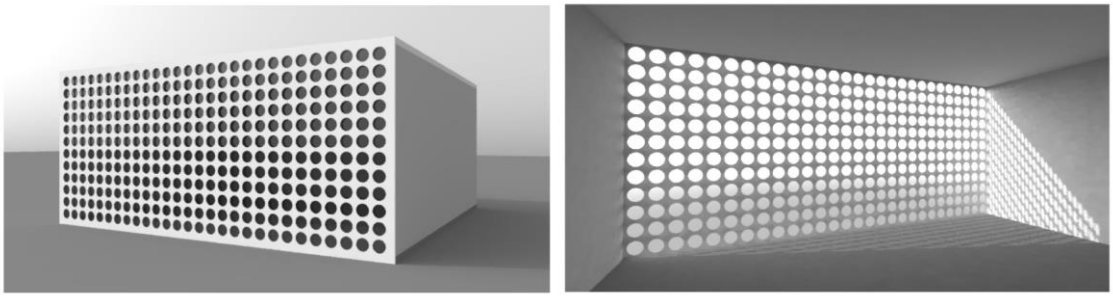

Figure 1. Rendering of a PSS example.

1.1 The issue of applying the building performance simulation tools

Several works have been devoted to the study of the thermal effects of fixed shading systems, such as louvres, overhangs and vertical fins [8,9] using EnergyPlus, TRNSYS and EES software for energy simulations [3]. A few works have reviewed the impact of perforated screens on reducing air conditioning and overheating, but these were developed for desert climates and for studying single design variables such as perforation range [10,11].

The impact of perforated façades on daylighting has, apparently, not been widely studied. There are few detailed studies regarding their effects on indoor illuminances by means of measurements on scale models [6,12,13] and computer simulations with Daysim and DIVA software [1,14,15]. Furthermore, these works addressed single design variables, such as shape [1,16], perforation rate and orientation [14] independently of each other.

A limited number of studies have addressed the balance between providing daylight and reducing solar gains derived from using solar control systems. Only a few relevant references exist [17,18]. This lack of studies addressing the integration of the daylighting and energy performances of PSS is due to the fact that such studies are complex tasks since these domains interact at many levels and simulation tools usually specialise in one domain only. The combination, therefore, of daylight and energy performance needs to employ different software packages in order to perform such detailed calculations. Moreover, to obtain accurate results building environmental performance simulation tools require a considerable amount of time and iterations. In addition, PSS usually present complex geometries, making them difficult to model in the current energy performance simulation tools and thus the design process becomes more sophisticated [19].

EnergyPlus, for example, is a whole building energy simulation program used to model the energy consumption in buildings – for heating, cooling, ventilation, lighting and other loads [20]. This software is well-suited to assessing the energy performance of conventional building systems or whole buildings, yet it is questionable whether such a tool can describe accurately the energy transfer phenomena that occur in complex geometries [21]. Furthermore, EnergyPlus has shown significant shortcomings in predicting the daylight available in a space, especially as the distance from the façade increases [22]. EnergyPlus utilizes the split flux method to model the interior reflections of light by dividing the luminous flux into two components; then, each split component is reflected by an average weighted reflectance of the surfaces above and below the window [20]. This kind of calculation often results in substantial inaccuracies that have direct consequences on electric lighting use intensity [23].

In order to overcome the simulation tools' limitations, some authors have developed methods using recent advances in software and/or in integrating the use of various software packages. Lagios, Niemasz and Reinhart [24] linked Rhinoceros/Grasshopper to Radiance/Daysim in order to evaluate key design parameters, such as window size and material descriptions. Azadeh [25] proposed a process for utilising daylighting and energy analysis software for optimising the performance of a sun-shading screen. To further understand the available daylight in the test space, a climate-based metric was calculated in DIVA. In order to model the effect of the screen on the energy consumption, the screen's hourly shading coefficient was calculated. An electric lighting schedule for the year was then generated and loaded into Design Builder for thermal simulations.

González and Fiorito [26] integrated parametric design with performance simulation tools. They used Galapagos/Grasshopper to define randomly the set of tests and then used DIVA both to calculate daylight metrics and to create an artificial lighting schedule. Finally, they used the DIVA thermal component to calculate the energy consumption and CO_2 emissions. Trubiano et al. [27] integrated the use of Grasshopper with Radiance and EnergyPlus through Matlab. Adopting genetic algorithms and a single objective function, they developed an evolutionary optimisation script to demonstrate the possibility of generating the optimal shape of atriums. Lobaccaro et al. [28] applied a similar method for optimising the geometry of a building in order to maximise the envelope's annual exposure to solar radiation. David et al. [29] applied the combination of daylight and thermal analysis for assessing solar shade efficiency. In order to rate the performance of different typologies of external overhangs, they used Radiance and EnergyPlus to calculate the shading coefficient, cooling energy demand, daylight autonomy, sun patch index and useful daylight illuminance.

1.2 The design optimisation problem

The optimisation problem, related to the design of external shadings in an office building, is linked to the time required for performing daylight simulations. This has been demonstrated to be about 35 times longer than that required for performing a full thermal dynamic analysis. Consequently, the feasibility of conducting an optimisation process for large areas or complex geometries is limited, especially when time is a constraint [26]. Furthermore, PSS design requires a wide variety of variables to be taken into consideration, so a comprehensive study of possible variable combinations requires a large amount of different models, simulations and time, something which is difficult to manage.

The Design of Experiments using Orthogonal Arrays (DOA) statistical method can simplify the interrelated study of a large number of variables, reducing the number of experiments/simulations and obtaining the maximum information which may be of use in PSS design [30]. The DOA method has been used efficiently in different fields of science, contributing valid conclusions and optimising processes [31]. It has been used to optimise building shape design in order to achieve energy savings [32] and to reduce construction costs [33]. It has also been used to optimise some window design parameters aimed at improving daylighting and solar control [34] and at maximising energy savings [35]. Chi, et al. [36] propose a methodology for applying orthogonal arrays (OA) to optimise the perforation percentage, shape, matrix and orientation of perforated screens, reducing the number of simulations from 256 to 16 and obtaining the best combination of variables for improving daylighting.

1.3 Aims of current research

As the energy demand of a building is greatly influenced by the levels of daylight and solar radiation entering through the perforations, enhancing daylighting and reducing solar gains are important considerations in PSS design. This paper aims to study the simultaneous taking into account of both daylighting and thermal performance of PSS to achieve the annual overall balanced solution. A workflow is proposed to integrate the use of daylighting and energy simulation packages to characterise and quantify the global performance of PSS. As, these studies are often complex and time-consuming due to a large number of simulations, this approach uses the DOA method to predict the optimal design derived from the combination of different PSS design variables such as perforation percentage (PP), matrix (M) and shape (S). The optimised PSS aims to find the right balance between the daylight availability and the reduction of the total energy consumption (lighting plus heating and cooling) for a typical office space in Seville, Spain.

2. Methodology

The proposed methodology consists of four main phases. First, the DOA method is applied to study simultaneously the interrelation of the PSS design variables and to reduce the number of study models. The second stage includes the parameters, performance metrics and software used for daylighting evaluation. The next phase includes an energy consumption calculation process by using different computer programs. Finally, a balanced solution, where the daylighting and thermal performance are considered, is identified. The required steps are summarised in Figure 2 and developed in more detail in the case study.

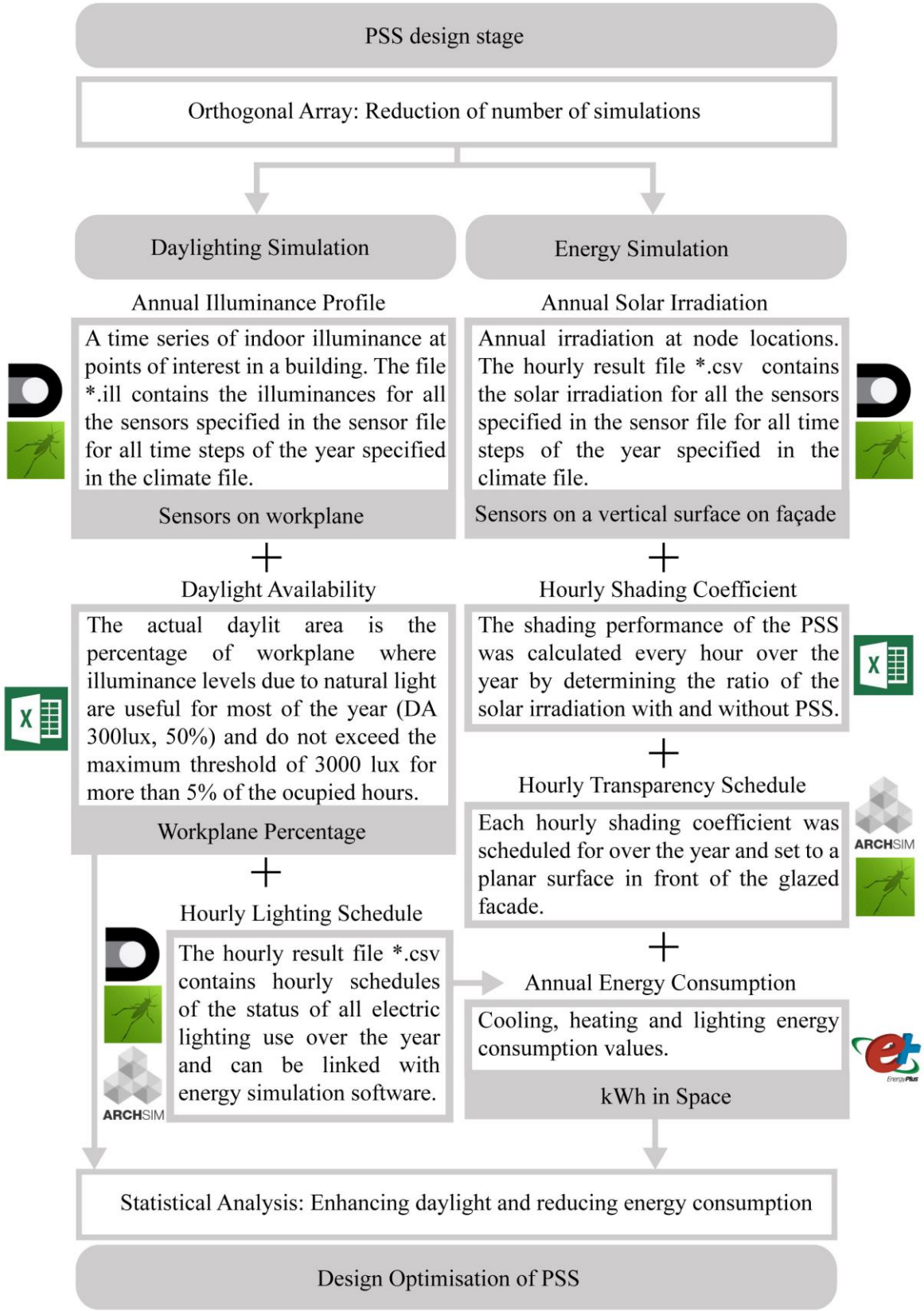

Figure 2. Workflow for daylighting and energy analysis of complex geometries.

2.1 Case study

The optimal PSS configuration for an open-plan office space located in Seville, Spain is investigated. A reference model measuring 7 m × 7 m and 3 m in height was modelled by using Rhinoceros software. It is a space that is sidelit through a fully-glazed, south-facing façade. Table 1 summarizes the model characteristics and materials that are set up according to the study domain. Namely, visible reflectances for daylighting calculations [37]; solar reflectances for annual solar radiation calculations [37]; and thermal properties for energy simulations [38]. These values remain fixed in all simulations in order to dismiss their effects on results.

Table 1. Characteristics of the internal model surfaces, PSS and glazing.

Wall	Visible reflectance	50%
	Solar reflectance	50%
	Material	Adiabatic
Floor	Visible reflectance	20%
	Solar reflectance	20%
	Material	adiabatic
Ceiling	Visible reflectance	80%
	Solar reflectance	80%
	Material	adiabatic
Glazing	Visible transmittance	78.1%
	Solar transmittance	60.4%
	Solar Heat Gain Coefficient (SHGC)	0.703
	Thermal Transmittance (U-value)	2.785 W/m^{2}K
PSS	Visible reflectance	90%
	Solar reflectance	90%
	Material	White Paint finish

2.2 PSS design

PSS are externally mounted at a distance of 0.05 m from the reference model's fully-glazed façade (Figure 1). The PSS dimensions are 7 m wide × 3 m high; the thickness is not considered. Characteristics of the PSS material are summarised in Table 1. Three design variables that are usually determined at the conceptual design stage are selected to characterise and evaluate the PSS performance:

(1) PP: Ratio of the total surface of the openings to the opaque surface.
(2) M: Vertical × horizontal distribution of openings on the screen. The distance between openings for each matrix is of 0.25, 0.33, 0.50 and 1.00 m, respectively, measured from the centre and vertically and horizontally equidistant.
(3) S: Four regular shapes are proposed. The different-shaped openings have the same opening area when M and PP are the same.

Figure 3 shows the levels for each design variable, together with their nomenclature between

parentheses which is used to name the PSS derived from the combination of the variables. For example, a PSS with a PP 37.5%, M 9×21 and S circular is named 372CS, where S is referring to the south. The reference model is termed REF100S, where 100 is referring to WWR (window-to-wall-ratio) 100%.

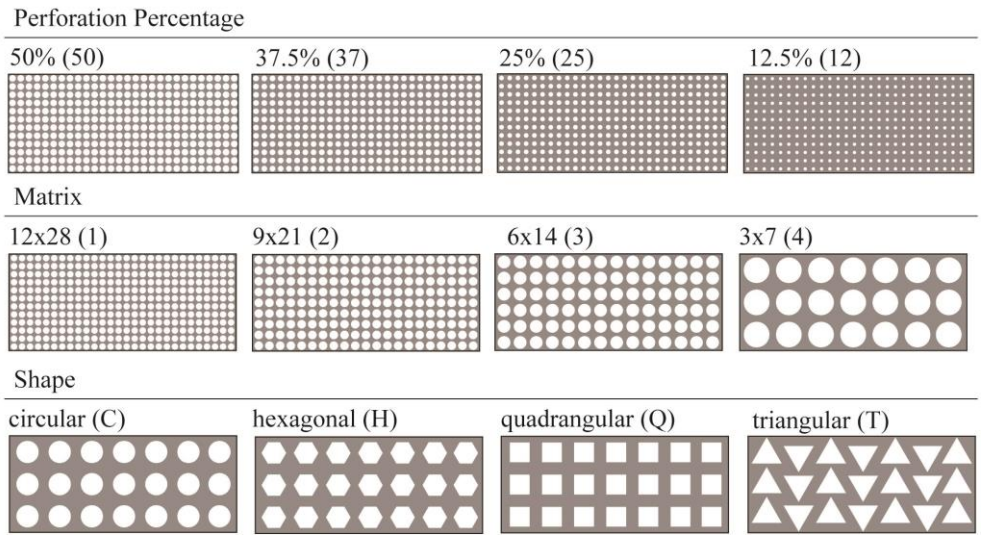

Figure 3. PSS design variables.

2.3 Orthogonal Array

All combinations of the four levels of the factors produce 64 PSS configurations, that is to say, 64 computer simulations need testing in different computer programs in order to obtain a simultaneous evaluation of daylighting and solar gains. This implies an increase in the number and time of simulations which can be difficult to handle in practical situations. There is a need, therefore, to propose an effective strategy for addressing multiple performance criteria, finding close-to-optimal solutions in a short period of time and with the minimum number of simulations.

To achieve this, the present paper uses the DOA method, validated in a previous study [36], in which some PSS design variables were analysed in terms of daylighting performance. The DOA method selects a representative fraction of all possible combinations of factors with the aim of distributing the experiments uniformly within the test range, accurately representing the overall situation [39]. The advantages of the DOA method are that the number of trials needed to complete the experiment is relatively small and the test results can be analysed through mean analysis (ANOM) and variance analysis (ANOVA). The method is highly efficient for arranging multi-factor experiments with optimal combination levels [40].

In DOA the experiment selection is OA-based, represented by a matrix which is expressed as $L_N (l)^k$, where L is OA, $_N$ the number of experiments, l the level of factors and k the number of factors or columns [30]. Many standard OAs have been tabulated for using DOA [39]. One of these arrays can be used directly for planning the simulation cases. It consist of three factors with four levels each: $L_{16}(4^3)$. The factors constitute the PSS design variables and the levels are the values of these variables, as summarised in Table 2.

Table 2. Factors and levels of L16(43).

Levels	Factors		
	1 (PP)	2 (M)	3 (S)
1	50%	12x28	Circular
2	37.5%	9x21	Hexagonal
3	25%	6x14	Quadrangular
4	12.5%	3x7	Triangular

$L_{16}(4^3)$ uses only a fraction of the possible 64 combinations of the three factors with four levels each ($4^3=64$ runs), reducing to 16 the number of PSS to be tested. Table 3 presents the 16 PSS configurations, which were obtained using a statistical analysis program [41].

Table 3. Simulations required in L16(43).

Simulation	PSS	Factors		
		1 (PP)	2 (M)	3 (S)
1	501CS	1 (50%)	1 (12x28)	1 (Circular)
2	502HS	1 (50%)	2 (9x21)	2 (Hexagonal)
3	503QS	1 (50%)	3 (6x14)	3 (Quadrangular)
4	504TS	1 (50%)	4 (3x7)	4 (Triangular)
5	371HS	2 (37.5%)	1 (12x28)	2 (Hexagonal)
6	372CS	2 (37.5%)	2 (9x21)	1 (Circular)
7	373TS	2 (37.5%)	3 (6x14)	4 (Triangular)
8	374QS	2 (37.5%)	4 (3x7)	3 (Quadrangular)
9	251QS	3 (25%)	1 (12x28)	3 (Quadrangular)
10	252TS	3 (25%)	2 (9x21)	4 (Triangular)
11	253CS	3 (25%)	3 (6x14)	1 (Circular)
12	254HS	3 (25%)	4 (3x7)	2 (Hexagonal)
13	121TS	4 (12.5%)	1 (12x28)	4 (Triangular)
14	122QS	4 (12.5%)	2 (9x21)	3 (Quadrangular)
15	123HS	4 (12.5%)	3 (6x14)	2 (Hexagonal)
16	124CS	4 (12.5%)	4 (3x7)	1 (Circular)

2.4 Daylighting Simulation

The aim of this stage is to investigate the daylighting performance of the PSS. The 16 daylighting simulations are performed with DIVA-for-Grasshopper [42]. DIVA is a highly-optimised daylighting and energy modelling plug-in for Rhinoceros. It comes with an enhanced user interface for Grasshopper, a graphical algorithm editor that enables designers with no formal scripting experience to generate parametric forms [43] rapidly. Grasshopper components [42] provide daylight analysis through Radiance/DAYSIM and thermal analysis through EnergyPlus/Archsim.

DAYSIM is a Radiance-based daylighting software that employs a reverse raytracing algorithm based on the physical behaviour of light in a volumetric, three-dimensional model [44]. It employs Daylight Coefficients method and Perez All-weather sky model to calculate the annual amount of illuminances and irradiances in and around buildings [45,46]. Radiance is a validated backward raytracer capable of simulating complex geometries with flexible reflection and transmittance material properties [47]. Its scientific reputation is further founded on a series of independent validation studies, which have demonstrated that Radiance is capable of modelling interior illuminances and irradiances for a wide range of sky conditions, a wide range of diffuse and specular reflecting real world materials, standard glazing and complex façade geometries [45,48,49].

2.4.1 Annual Illuminance Profile (.ill)*

The calculation of the time series of daylight illuminances at sensor points requires the project location to be specified. Here, the weather file used is IWEC for Seville, Spain (37°42'N, 5°9'W). The daylighting test is conducted on a workplane 0.80 m above the floor, with 576 sensor points arranged in a grid of 0.25 × 0.25 m, as Figure 4 shows. The daily occupancy hours of a typical office space is used (8-18 h, from Monday to Friday). Radiance simulation parameters are specified in Table 4. After DIVA simulations, an annual illuminance profile (*.ll) is generated and subsequently used to calculate mathematically the daylight performance indicators.

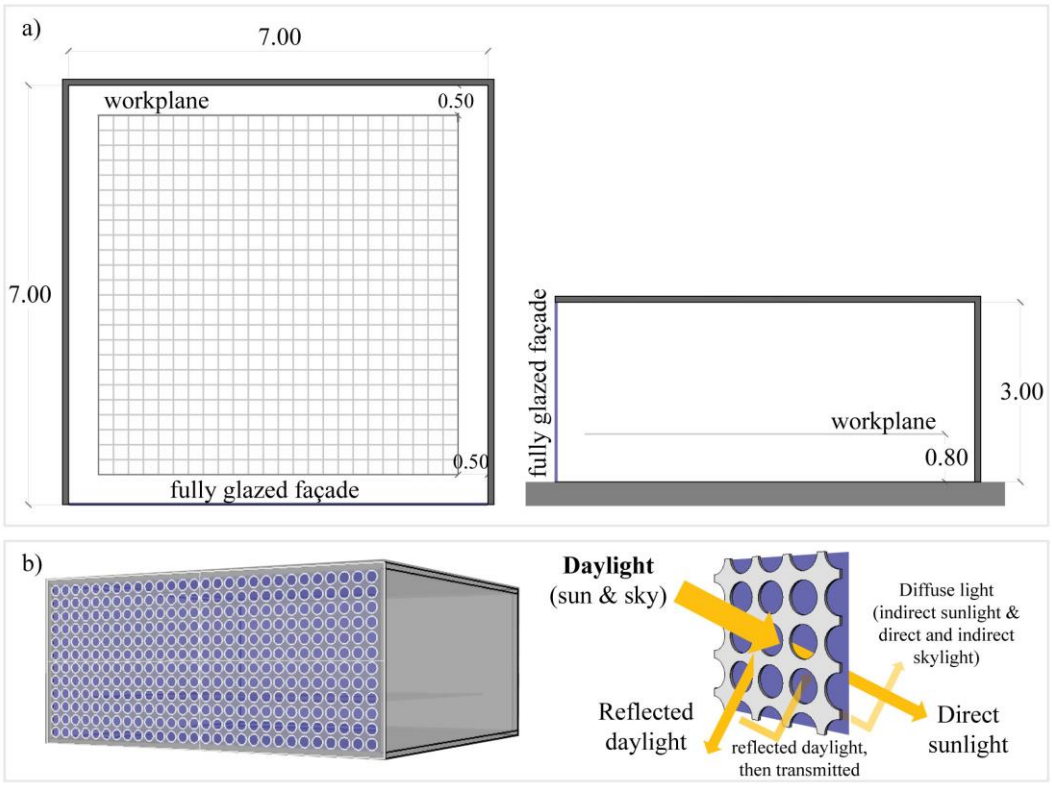

Figure 4. Daylight model: a) Reference, and b) PSS example with a schematic diagram showing the visible light entering.

Table 4. Radiance parameters

Ambient bounces	Ambient division	Ambient sampling	Ambient accuracy	Ambient resolution	Direct threshold	Direct sampling
7	1500	100	0.1	300	0	0.2

2.4.2 Modified Daylight Availability

The daylighting criteria used for assessment are based on Daylight Availability [50]. Through this metric, the space area is represented as follows: 'fully daylit', 'partially daylit', 'overlit' and 'non-daylit' areas. The 'fully daylit' area is reported when a specified illuminance level (300 lux) for occupancy from 8 to 18 h is over 50% (in short, $DA_{300,50\%}$). The 'partially daylit' area is measured when a specified illuminance level (150 lux) for occupancy from 8 to 18 h is at least 50% (in short, $DA_{150,50\%}$) [50]. The 'overlit' area is reported when daylight illuminance exceeds the maximum threshold of 3000 lux for more than 5% of the occupied hours. This area might signify a potential for glare and heat gain [51,52]. The 'non-daylit' area is that which did not achieve the illuminance level of 150 lux for at least half of the occupied hours.

From the above, it can be determined that the 'fully daylit' area is part of the 'partially daylit' area since they do not have upper limits [53]. In addition, the 'overlit' area could be coincident with and/or contained within any/all three other areas. Notwithstanding, this work aims to account the space area lit exclusively with useful daylight illuminance (UDI) levels by means of assessing the annual occurrence of illuminances across the workplane that are within a range that occupants considered 'useful'[54]. Accordingly, the four Daylight Availability areas are overlapped on top of each other in order to extract the single area for each one of them, as Table 5 indicates:

Table 5. Modified Daylight Availability

Non-daylit	includes illuminances of under 150 lux for at least 50% of occupied hours ($UDI_{<150,\ \geq 50\%}$).
Actual Partially daylit	is measured when daylight illuminances fall within the range 150-300 lux for at least 50% of occupied hours ($UDI_{150\text{-}300,\ \geq 50\%}$).
Actual daylit	includes only those useful illuminances within the ranges $UDI_{300\text{-}3000,\ \geq 50\%}$ + $UDI_{>3000,\ <5\%}$.
Overlit	includes illuminances of over 3000 lux for at least 5% of the occupied hours ($UDI_{>3000,\ \geq 5\%}$).

Therefore, non-daylit + actual partially daylit + actual daylit + overlit areas = 100% of the workplane, as Figure 5 shows. These areas are obtained by mathematically processing the information of the annual illuminance profile using Excel software, because DIVA/Grasshopper cannot calculate the illuminance ranges in the specific time percentages required in this work.

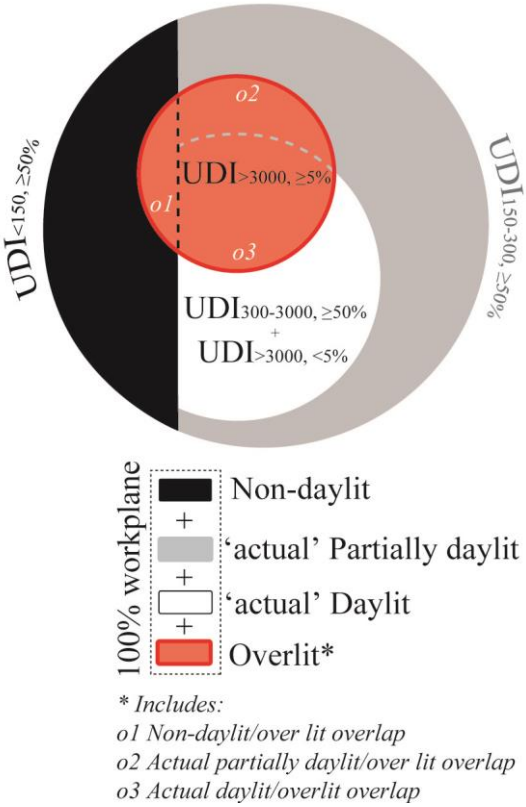

Figure 5. Modified Daylight Availability.

2.4.3 Hourly Lighting Schedule

DIVA includes a module that enables users to model annual electric lighting use based on Radiance backward raytracing. The resulting file (*.csv) contains hourly schedules of the status of all lighting systems in the project. This schedule can be linked to energy simulation programs such as EnergyPlus. Three parameters are required to describe the lighting system for each zone: the target illuminance, the lighting power density and the lighting control system. The former is set to 300 lux (IESNA 2013) and the latter to 10.6 W/m^2 (ASHRAE 2016). The lighting system selected corresponds to a standard, manually-controlled electric lighting system with a single on/off switch near the door. This manual on/off switch mimics the behaviour of a user based on the statistical analysis of the Lightswitch Study [57] where users occupying a space are likely to turn off lights at levels of around 250 lux. According to the IESNA (2011), this is the reference system relative to which the energy savings potential of automated controls should be expressed.

2.5 Energy Simulation

The aim of this stage is to evaluate the thermal performance of the office space with the 16 PSS configurations selected by the DOA method. Currently, energy calculation presents some difficulties and restrictions due to the simulation tools' limitations. EnergyPlus is an energy simulation program

that has been thoroughly validated and tested in practice in order to assess the energy performance of conventional building systems [56]. It is one of the newest and most advanced building energy simulation programs and it is the energy modelling engine that the US Department of Energy is betting the future of building modelling on. However, it is questionable whether it can describe accurately the energy transfer phenomena that occur within the complex geometries [21]. Even its different graphical interfaces (such as Design Builder and DIVA-thermal component) cannot deal well with such geometries, making the energy evaluation of PSS infeasible [25].

This paper proposes an energy calculation process that integrates the advantages of EnergyPlus with the full potential that other simulation tools have developed in terms of modelling and characterising complex geometries such as Radiance, Archsim and Grasshopper [48,59,60]. In order to model the thermal performance of the PSS, a specific calculation process is developed (Figure 2). First, DIVA-for-Grasshopper is used to calculate an annual solar irradiation profile. This profile is then synchronised with a thermal analysis performed in Archsim/Grasshopper linked with EnergyPlus by using an hourly shading coefficient and an hourly transparency schedule. The entire process is detailed below.

*2.5.1 Annual Solar Irradiation Profile (*_hourlyirradiation.csv)*

Climate-specific annual solar irradiation is calculated with DIVA using the DAYSIM-based hourly method to produce an hourly result file (*_hourlyirradiation.csv) containing the solar irradiation for all of the sensors for all of the hours in the year. Solar irradiation is measured on a vertical plane placed in front of the glazed façade, with 2,201 sensor points arranged in a grid of 0.10 × 0.10 m, as Figure 6 shows. Radiance simulation parameters are presented in Table 2. The weather file is IWEC for Seville.

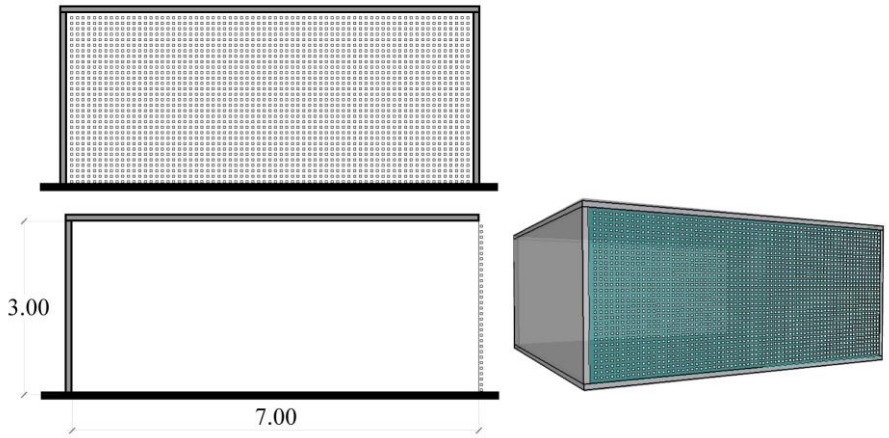

Figure 6. Reference model with the solar irradiation grid: Façade, section y perspective.

2.5.2 Hourly shading coefficient

Shading Coefficient (SC) enables the performance of the solar protection over glazing to be

determined. It is merely the fraction of the solar irradiation that impacts the glazing with and without the use of solar shadings; the closer the SC is to 0, the more effective the solar protection is [61]. SC could be taken to represent the thermal efficacy of the solar shades [29]. In this work, the SC is calculated for every hour over the year (SC_{hourly}) and is the ratio of the solar irradiation falling on the grid with and without PSS (See Figure 7). Each value of SC_{hourly} considers the mean across all sensors in the grid. Thus, 8,760 values of SC_{hourly} are obtained for each PSS configuration.

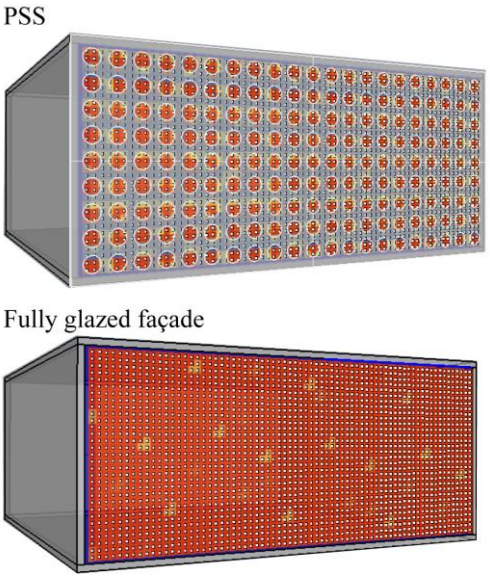

Figure 7. Solar irradiance with and without PSS.

2.5.3 Hourly Transparency Schedule

Since the creation of Grasshopper, several scripts have been developed aimed at integrating simulation tools for different aspects of building performance, such as, but not limited to: geometry, structures, thermal and daylight performance [26]. One example of these scripts is Archsim Energy Modelling [60], a plugin that brings fully-featured EnergyPlus simulations to Rhinoceros/Grasshopper and thus links the EnergyPlus simulation engine with a powerful parametric design and a CAD modelling environment. Thermal analyses with EnergyPlus can thus be accessed by a wider range of users. Through Archsim, simulation inputs such as model geometry, materiality, constructions and zone usage profiles are fully parametric and can be coupled with optimisation algorithms within Grasshopper [43,62]. Archsim supports advanced daylighting and shading controls, ventilation modules, simple HVAC, etc.

In this work, Archsim is used to create an 'hourly transparency schedule' with the 8760 SC_{hourly} values, for each one of the 16 PSS studied. Figure 8 shows an example of this hourly transparency schedule over the year.

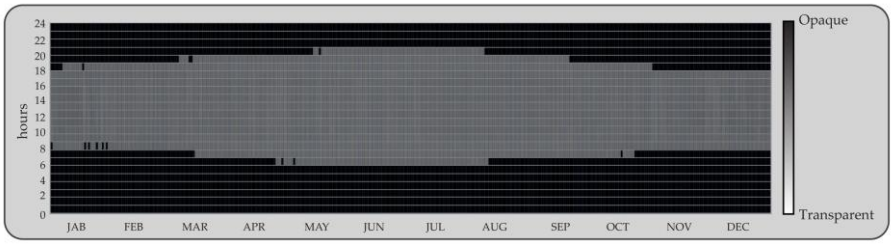

Figure 8. Example of an hourly transparency schedule.

2.5.4 Annual Energy Calculation

The thermal simulations are performed with EnergyPlus version 8.4.0. As EnergyPlus is a stand-alone simulation program without a user-friendly graphical interface, Archsim intervenes, enabling designers to set up and run energy models rapidly. In order to focus on studying the performance of the tested PSS, the effect of thermal transmittance through walls, ceiling and floor was set to be adiabatic, which is fully-glazed with clear double glazing (6mm), separated by a 13 mm air gap, with a U-value of 2.785 W/m^2-K and SGHC of 0.703. A single-plane surface measuring 7 m $\times$ 3 m is placed at a distance of 0.05 m from the fully-glazed façade. The hourly transparency schedules of the 16 PSS are individually set to this plane. Figure 9 depicts the basic thermal behaviour of the façade exposed to solar radiation.

The calculation method used for the thermal model in EnergyPlus is the Conduction Transfer Function (CTF) since it rapidly calculates the conduction heat transfer through a complete layered building surface. It has been pointed as the best choice for simulating peak cooling loads and for the building energy consumption simulation analysis [63]. The details of the CTF model can be found in [20]. Table 6 lists the occupancy, lighting and equipment loads [64]; also, the heating and cooling set points, relative humidity and other input loads based on Spanish regulations [38]. Table 7 lists the indicators quantified to understand the thermal performance of PSS.

Table 6. Input loads for thermal dynamic simulations

Occupancy	0.1 people/m^2
Equipment loads	12 W/m^2
Lighting loads	10.6 W/m^2 (It is set to be manually controlled according to the DIVA hourly lighting schedule)
Heating set point temperature	21°C
Cooling set point temperature	25°C
Minimum relative humidity	45%
Maximum relative humidity	50%
Fresh air	12.5 L/s/person
Sensible heat recovery	0.64
Infiltration	Off

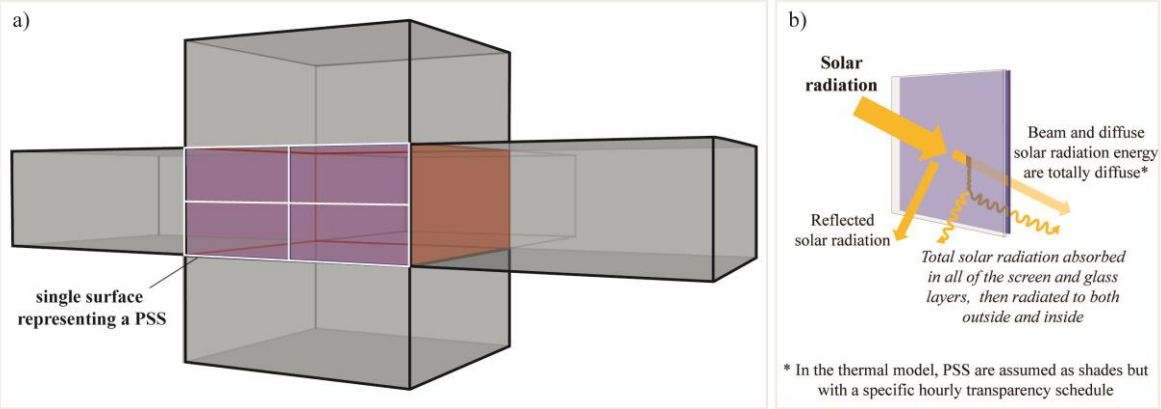

Figure 9. Thermal model: a) 3D geometry, and b) Basic thermal behaviour.

Table 7. Energy performance indicators

SC_{annual}		Annual mean value of all SC_{hourly} values quantified at each PSS.
TSRE		Annual transmitted solar radiation energy, normalised by floor area (kWh/m^2).
Lighting energy consumption		Total annual energy used on-site to supply the electric lighting system and normalised by floor area (kWh/m^2).
Cooling energy consumption		Total annual energy used on-site to supply the cooling system and normalised by floor area (kWh/m^2).
Heating energy consumption		Total annual energy used on-site to supply the heating system and normalised by floor area (kWh/m^2).
Total Energy Consumption		Sum of the annual energy consumed for heating, cooling and artificial lighting and normalised by floor area (kWh/m^2).

2.6 Balancing daylighting and thermal performance

The ratio of the actual daylit area to the SC_{annual} is counted as an index of both daylighting and solar shading in this study [34]. A high value of the actual daylit area corresponds to better daylighting performance. A lower SC_{annual} value corresponds to better annual solar shading performance; thus, high values of this index represent a better integrated performance of solar shading and daylighting.

3. Results

Table 8 and Figure 10 present the annual results of the 16 simulations. Figure 10a shows the percentages of the modified Daylight Availability and Figure 10b shows the annual energy used for lighting, cooling and heating, the SC_{annual} and the TSRE. The index appears in both figures a and b to show the interrelation between the daylighting and thermal performance.

Table 8. Annual results of simulations.

Simulation	PSS	Non-daylit area (%)	Actual Partially daylit area (%)	Actual Daylit area (%)	Overlit area (%)	Annual Solar Radiation on Façade (kWh/m^2)	SC_{annual}	TSRE (kWh/m^2)	Lighting energy (kWh/m^2)	Cooling energy (kWh/m^2)	Heating energy (kWh/m^2)	Index
-	REF100S	0	0	0	100	1147.04	1.00	289.29	9.21	248.62	4.66	0.00
1	501CS	0	0	43	57	726.78	0.70	154.28	13.39	138.71	1.50	0.61
2	502HS	0	0	42	58	646.41	0.59	140.27	21.24	134.11	1.27	0.72
3	503QS	0	0	43	57	707.90	0.68	150.91	21.96	143.11	1.55	0.63
4	504TS	0	0	45	55	669.78	0.60	145.81	13.07	131.98	1.34	0.75
5	371HS	0	0	49	51	596.91	0.60	127.75	23.59	126.25	1.05	0.82
6	372CS	0	0	49	51	515.53	0.48	113.66	24.78	116.67	0.81	1.02
7	373TS	0	0	47	53	532.78	0.51	116.68	16.89	112.62	0.79	0.92
8	374QS	0	0	50	50	471.36	0.42	106.19	14.92	103.81	0.64	1.20
9	251QS	0	36	23	41	381.95	0.37	86.56	26.24	98.85	0.54	0.63
10	252TS	0	34	23	43	392.84	0.39	88.37	25.82	99.85	0.56	0.59
11	253CS	0	35	20	44	338.36	0.31	79.11	26.35	94.00	0.50	0.66
12	254HS	0	31	29	40	333.27	0.31	78.10	26.30	93.24	0.49	0.94
13	121TS	50	15	5	31	154.61	0.13	43.43	27.26	72.69	0.56	0.35
14	122QS	47	23	8	22	191.23	0.19	49.58	27.23	76.35	0.49	0.43
15	123HS	48	24	13	14	190.97	0.19	49.42	27.44	76.45	0.51	0.70
16	124CS	44	16	13	27	171.06	0.16	46.03	27.42	74.40	0.55	0.82

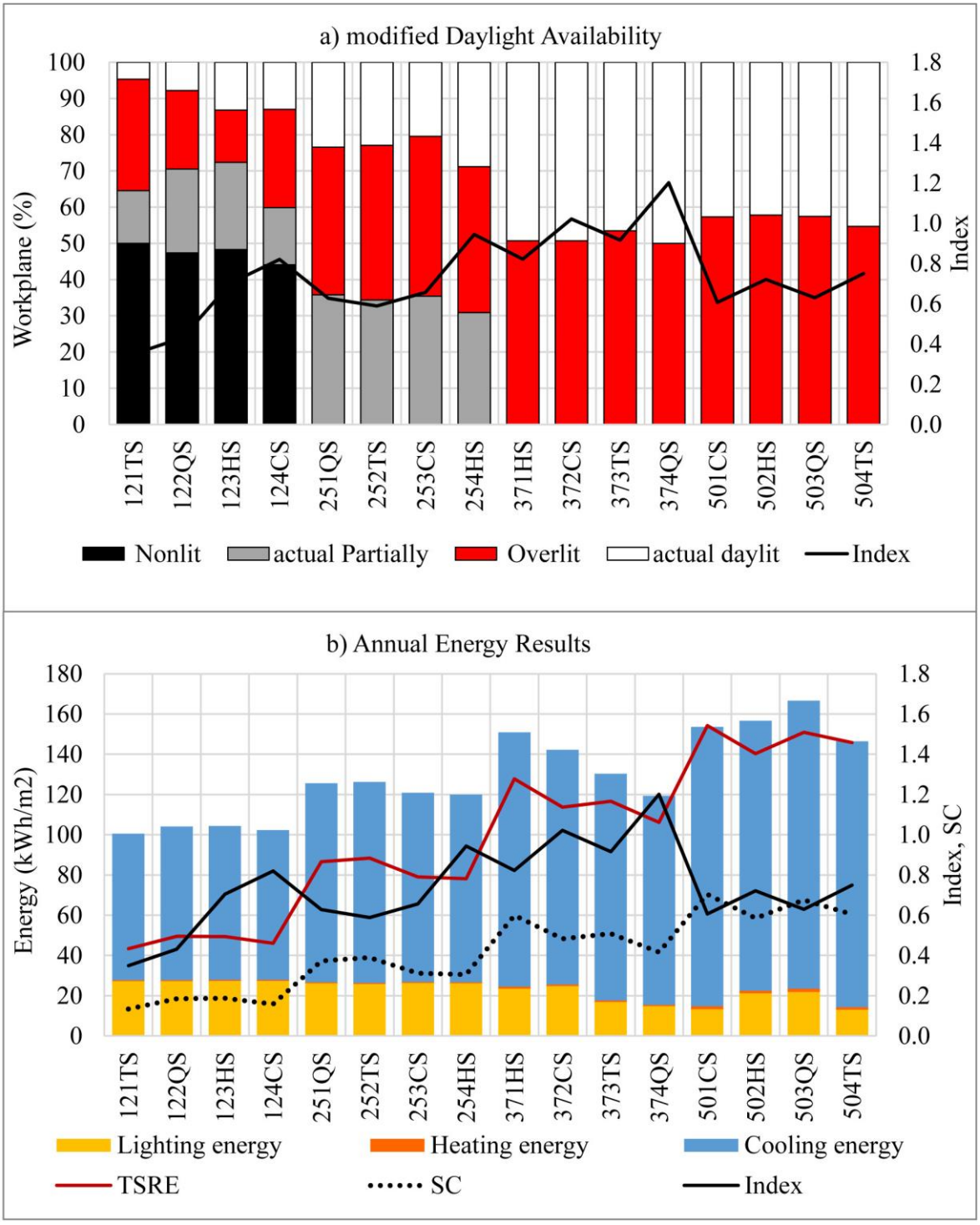

Figure 10. Annual Results in L16(43).

3.1 OA analysis

The ANOM and ANOVA of the OA $L_{16}(4^3)$ are used to predict the optimal design derived from the combination of the three design variables. The optimal levels, therefore, must increase the area lit with useful illuminance for occupants and reduce the area lit with excessive illuminance that can be associated with glare and thermal discomfort. The 'actual daylit area' must be maximised and the 'non-daylit', 'actual partially daylit' and 'overlit' areas must be minimised. Furthermore, the optimal levels must maintain electrical energy consumption for lighting, cooling and heating as low as possible. As it represents the best integrated performance of daylighting and solar shading, the index must be maximised.

Table 9 summarises the ANOVA results of $L_{16}(4^3)$, where the statistical significance to 5% is of PP for all indicators and M for the index. The sum of squares (SS) indicates the relative importance of each factor and is ordered as follows: PP>M>S for all indicators (except for the overlit indicator that follows the order PP>S>M).

Table 9. ANOVA of L16(43) when α=0.05

Indicator	Factor	GL	SS	F	*p*	Significance
Non-daylit area	1 (PP)	3	6751.44	1467.03	0.00	*
	2 (M)	3	4.60	1.00	0.46	
	3 (S)	3	4.60	1.00	0.46	
	Residual error	6	9.20			
	Total	15	6769.85			
'actual' partially daylit area	1 (PP)	3	3296.90	144.46	0.00	*
	2 (M)	3	27.12	1.19	0.39	
	3 (S)	3	14.22	0.62	0.63	
	Residual error	6	45.64			
	Total	15	3383.88			
'actual' Daylit area	1 (PP)	3	3868.34	254.39	0.00	*
	2 (M)	3	45.43	2.99	0.12	
	3 (S)	3	25.78	1.70	0.27	
	Residual error	6	30.41			
	Total	15	3969.96			
Overlit Area	1 (PP)	3	2559.32	48.43	0.00	*
	2 (M)	3	13.76	0.26	0.85	
	3 (S)	3	54.09	1.02	0.45	
	Residual error	6	105.70			
	Total	15	2732.88			
TSRE	1 (PP)	3	22480.90	152.38	0.00	*
	2 (M)	3	163.30	1.11	0.42	
	3 (F)	3	1.00	0.01	1.00	
	Residual error	6	295.10			

	Total	15	22940.20			
Lighting energy	1 (PP)	3	274.33	7.54	0.02	*
	2 (M)	3	38.61	1.06	0.43	
	3 (F)	3	30.49	0.84	0.52	
	Residual error	6	72.72			
	Total	15	416.15			
Cooling energy	1 (PP)	3	8363.61	80.35	0.00	*
	2 (M)	3	147.82	1.42	0.33	
	3 (F)	3	21.27	0.20	0.89	
	Residual error	6	208.18			
	Total	15	8740.88			
Heating energy	1 (PP)	3	2.12	49.83	0.00	*
	2 (M)	3	0.06	1.37	0.34	
	3 (F)	3	0.00	0.08	0.97	
	Residual error	6	0.08			
	Total	15	2.26			
Index	1 (PP)	3	0.38	18.86	0.00	*
	2 (M)	3	0.23	11.47	0.01	*
	3 (F)	3	0.05	2.57	0.15	
	Residual error	6	0.04			
	Total	15	0.70			

Table 10 presents the results of the $L_{16}(4^3)$ ANOM. Delta values are used to compare the relative magnitude of effects depending on orthogonal design [41]. It also shows the optimal PSS configuration which obtains the highest index values.

Table 10. $L_{16}(4^3)$ ANOM.

Mean values	Non-daylit area (%)	'actual' Partially daylit area (%)	'actual' Daylit area (%)	Overlit area (%)	TSRE (kWh/m2)	Lighting energy (kWh/m2)	Cooling energy (kWh/m2)	Heating energy (kWh/m2)	Index
PP									
T1 (50%)	**0**	**0**	43	57	147.82	**17.42**	136.98	1.41	0.68
T2 (37.5%)	**0**	**0**	**49**	51	116.07	20.04	114.84	0.82	**0.99**
T3 (25%)	**0**	34	24	42	83.03	26.18	96.49	**0.52**	0.70
T4 (12.5%)	47	19	10	**23**	**47.12**	27.34	**74.97**	0.53	0.58
Delta	47	34	39	33	101	10	62	1	0.41
Rank	1	1	1	1	1	1	1	1	1
M									147.82
T1 (12×28)	13	13	30	45	103.00	22.62	109.13	0.91	0.60
T2 (9×21)	12	14	31	43	97.97	24.77	106.75	0.78	0.69
T3 (6×14)	12	15	31	**42**	99.03	23.16	106.54	0.84	0.73
T4 (3×7)	**11**	**12**	**34**	43	**94.03**	**20.43**	**100.86**	**0.75**	**0.93**

Delta	1	3	4	2.52	9	4	8	0	0.33
Rank	2.5	2	2	3	2	2	2	2	2
S									
T1 (C)	**11**	13	31	45	**98.27**	22.99	105.95	0.84	0.78
T2 (H)	12	14	**33**	**41**	98.89	24.64	107.51	0.83	**0.80**
T3 (Q)	12	15	31	42	98.31	22.59	105.53	**0.80**	0.72
T4 (T)	13	**12**	30	45	98.57	**20.76**	**104.29**	0.81	0.65
Delta	1	2	4	5	1	4	3	0	0.15
Rank	2.5	3	3	2	3	3	3	3	3
Optimal PSS									374H

Note: the numbers in bold represent optimal levels according to the indicators.

Figure 11 presents the $L_{16}(4^3)$ ANOM. 10a plots the annual modified Daylight Availability where the non-daylit area can be observed to remain at zero in PPs larger than 25% and shows fluctuations that are broadly similar for all levels of M and S. The actual partially daylit area remains at zero for PPs greater than 37.5% and presents close fluctuations between levels M and S. The actual daylit area reaches its highest value at 37.5% PP, followed by 50% PP. It then decreases as PP decreases. This area shows a slight increase at levels 4 (3×7) for M and 2 (H) for S. The overlit area decreases as PP decreases and presents close results in all 4 levels of M and S.

Figure 11b plots the annual means of the PSS energy performance indicators. It can be observed that, similar to the overlit area, TSRE decreases as PP decreases; furthermore, it reaches highly similar values in M and S levels. SC_{annual} behaves the same as TRSE in the three design variables. Lighting energy increases slightly as PP decreases and presents fluctuations at levels M and S. Cooling energy decreases as PP decreases; moreover, it is lower in M4 (3×7) and presents fluctuations at S levels. Heating energy remains practically the same over all variables. With regard to the index, PP 37.5%, M 4 (3×7) and S 2 (C) and 1 (H) levels obtain the best simultaneous performances in the two aspects under study.

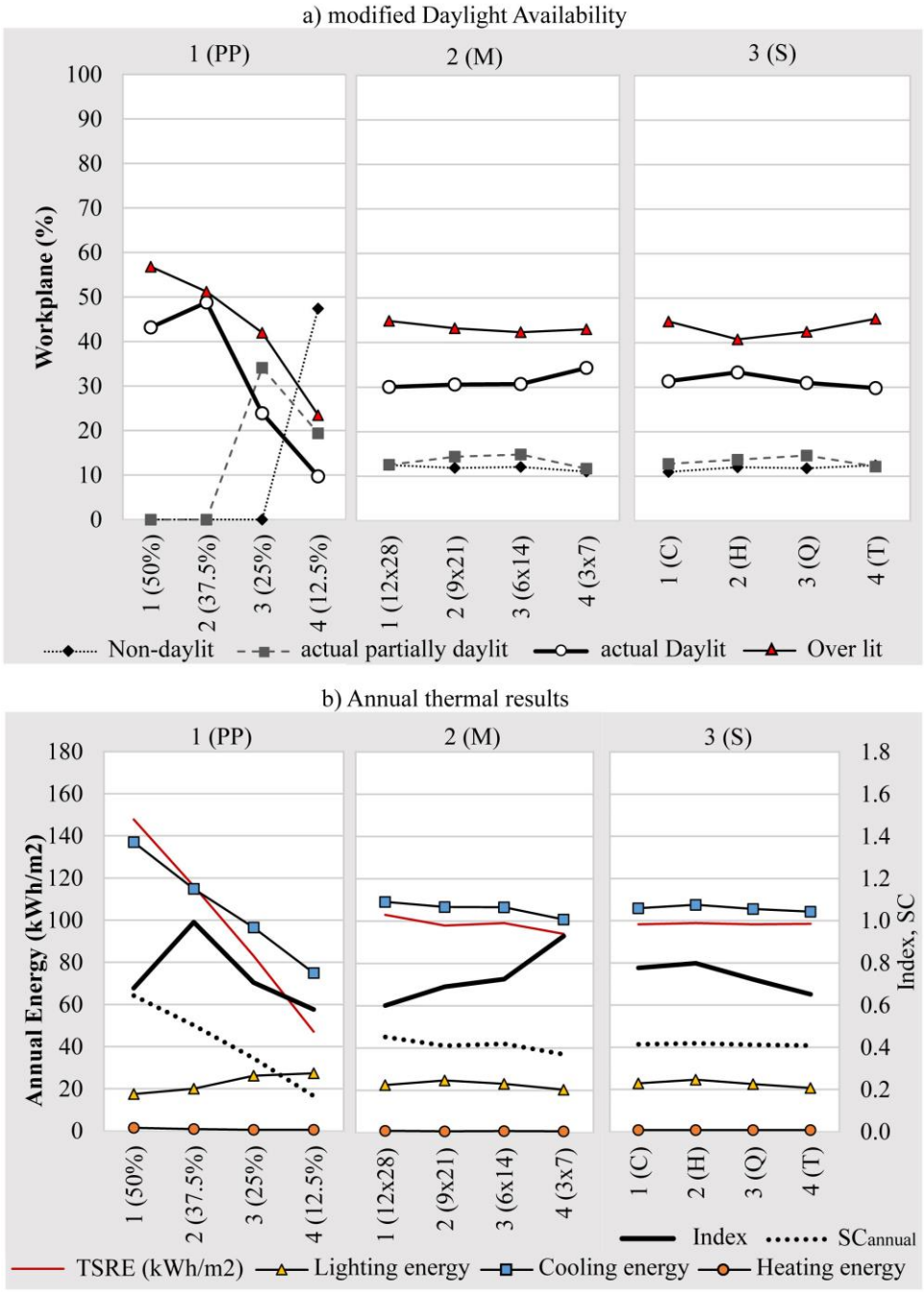

Figure 11. L16(43) ANOM results.

The index is used for the daylighting and thermal characterisation of the PSS and endeavours to find a balance between natural daylight and thermal efficiency. The following design criteria for south-facing, Mediterranean PSS have been derived from their optimal levels:

- PP is the determining variable in PSS design since it was statistically significant for all indicators. PP should be limited to 37.5% for the following reasons (See Table 10). In terms of daylighting performance, a PP of 37.5% gives the highest actual daylit area value (49%);

PPs greater than 37.5% increased the overlit area in more than 50% of workplane (57%), while PPs of less than 37.5% led to a considerable (10-24%) reduction. In terms of thermal performance, a PP of 37.5% gives intermediate values with respect to lighting, heating and cooling energy consumption, achieving annual savings when compared with larger PPs. The highest index value is obtained with PP 37.5% and therefore it is effective when describing simultaneously the PPs' daylighting and thermal performance.

- The second most important factor is the matrix. In order to achieve the best balance between daylight and energy performance, matrices with the smallest number of large perforations are recommended. According to the results in daylighting performance, level 4 (3x7) obtains the highest actual daylit area values, while in terms of the overlit area, all four levels are roughly equal, with levels 3 (6×14) and 4 (3×7) giving the lowest values. In terms of thermal performance, level 4 (3x7) is the most advisable because it achieves the lowest levels of energy consumption for all energy uses, as well as the lowest TSRE levels. With regard to the index, the optimal level is level 4 (3x7) and is therefore effective in characterising both conditions simultaneously. Even M is statistically significant for the index (See Table 9).
- Shape is the least relevant variable, allowing for greater design freedom. The results showed no significant differences in any indicator (See Table 9).

3.2 Analysis of the use and non-use of south-facing PSS

This section compares the space's daylighting and thermal conditions with and without PSS, selecting for that purpose configuration 374QS from the simulations that had already been performed. This configuration was chosen because it combines the optimal and statistically significant levels derived from the OA, as well as being the PSS with the highest index (See Figure 10). Figure 12a shows the absolute quantified error in 374QS with respect to REF100S for modified Daylight Availability, as well as the quantified percentual error for both energy consumption and TSRE. The results demonstrate that using optimised south-facing PSS can increase the actual daylit area by 50% and decrease the overlit workplane area by 50% when compared with a fully-glazed façade. Although with PSS artificial lighting consumption rises by 62%, daylighting on the workplane is improved considerably. Furthermore, there is a 63% reduction in TSRE while cooling and heating consumption decrease by 58% and 86%, respectively. This gives a 55% total annual saving in energy consumption. It is, therefore, advisable to use PSS on south-facing glazed façades in line with the abovementioned design criteria.

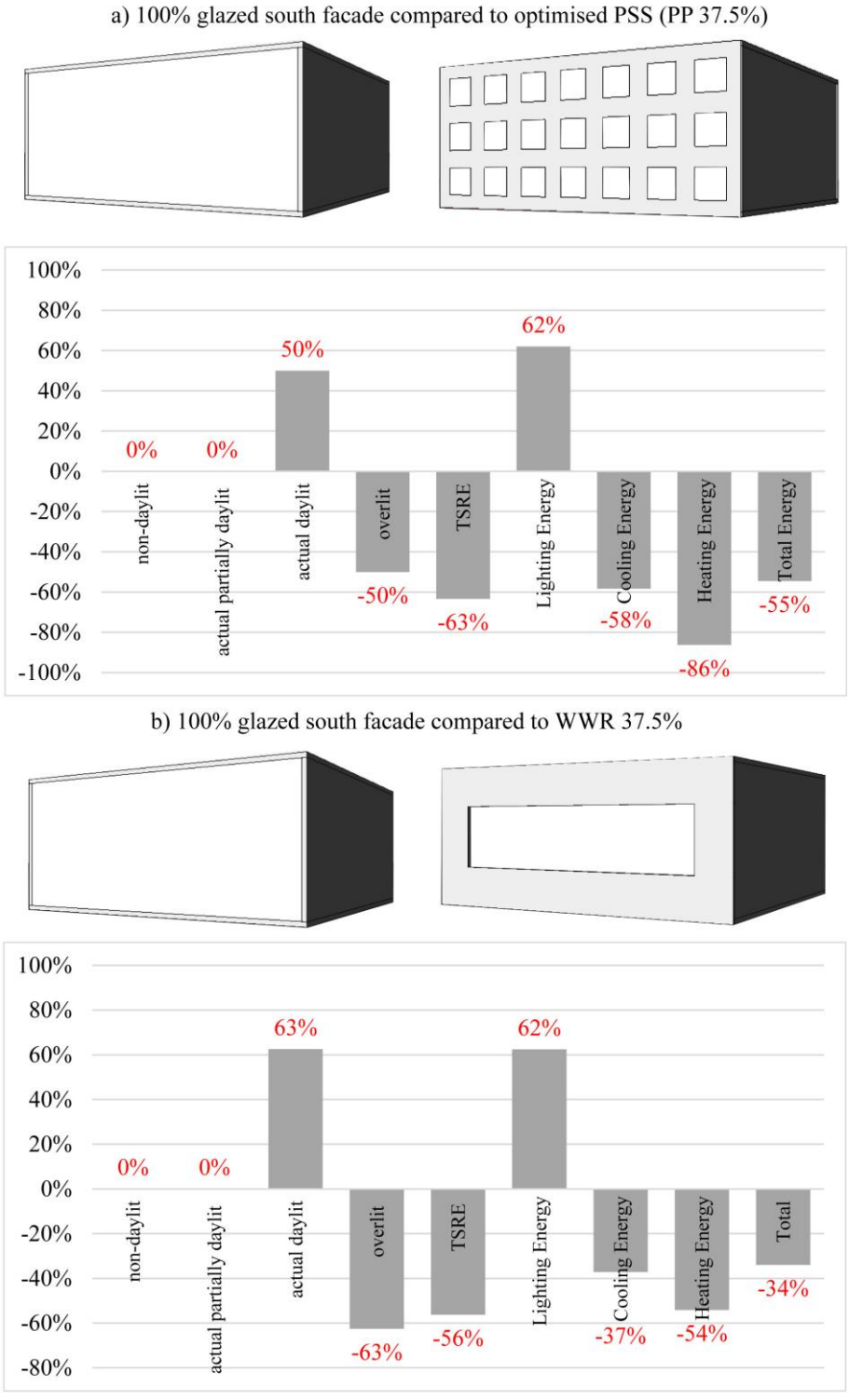

Figure 12. Differences between use and non-use of an optimised south facing PSS.

Figure 12b compares the daylighting and thermal performance of the optimised PSS with respect to a simple aperture with WWR 37.5%. The absolute error in 374QS with respect to WWR 37.5% for modified Daylight Availability is shown, as is the quantified percentual error in 374QS with respect

to WWR 37.5% for energy consumption and TSRE. The results show that using a simple aperture can increase the actual daylit area by 63% and reduce the overlit area on a workplane by 63% with respect to the fully-glazed façade. Artificial lighting consumption, however, increases by 62% which is similar when using PSS. Moreover, TSRE decreases by 56% and cooling and heating consumption by 37% and 54%, respectively. There is only a 34% decrease in overall energy consumption; 21% less than when using PSS. On balance, therefore, it is more advisable to use PSS on glazed façades instead of a simple aperture in the wall.

3.3 Characterisation of PSS daylighting and thermal performance

Figure 13 shows an overlap of the four areas of the modified daylight availability at each sensor point in 374QS. The white areas represent a sensor with DA_{300} for at least 75% of the working year that do not reach $UDI_{>3000}$ during 5% of the occupied hours (in short, the favourable actual daylit area). The clear grey scale shows sensors with DA_{300} between 50 and 75% of the working year that do not reach $UDI_{>3000}$ during 5% of the occupied hours (in short, the nominal actual daylit area). In addition, the REF100S results also appear in Figure 13 for in order to present daylight on the workplane without PSS. Not only can the daylighting improvement be observed in the increased actual daylit area but also in the reduction of the overlit area and, furthermore, in the reduction of the annual time percentages with excessive illuminances at each sensor point.

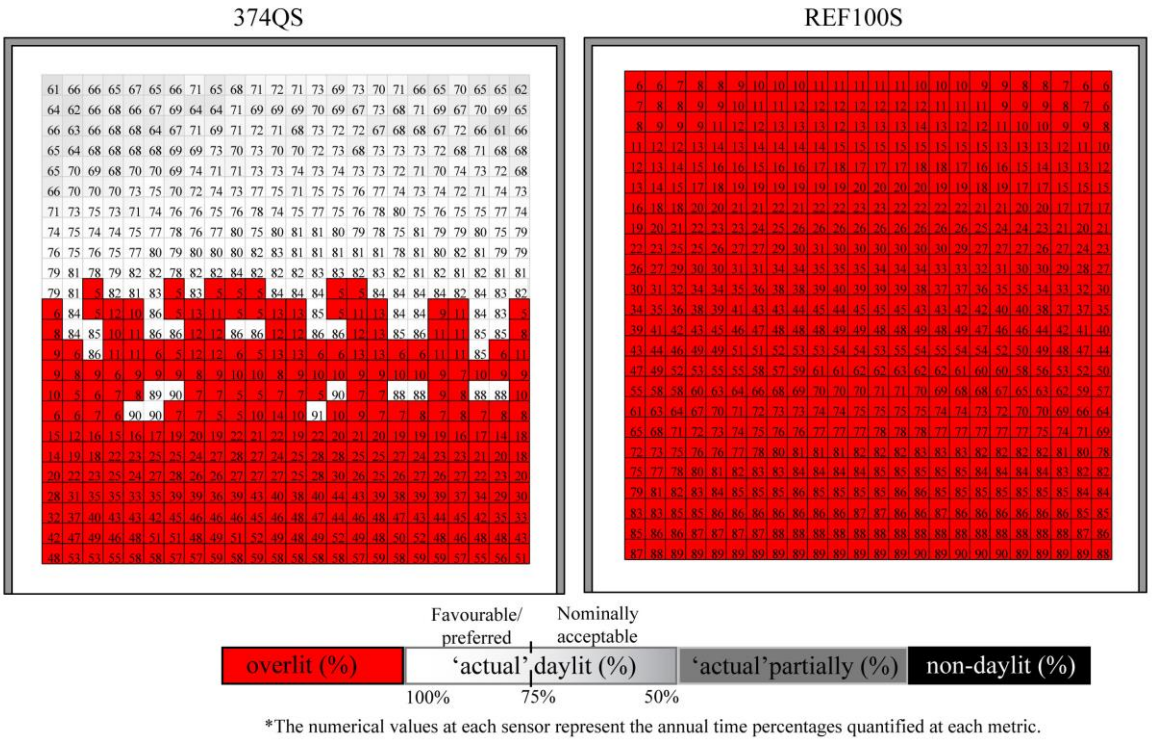

Figure 13. Daylight Availability in 374QS and REF100S.

In this work, illuminance and TSRE information are shown using annual temporal maps. These temporal maps are produced in MATLAB in order to show, on a single graph, the periods of the year

in which the design objectives are achieved [65]. The illuminance information can be coupled with studies for integrating daylight with dimmable artificial light. The TSRE information is useful to complement the PSS performance with dynamic solar protection systems during the hours of greatest sunlight gain. Figure 14a shows the temporal illuminance map of 374QS. It represents the percentage of the workplane fulfilling useful illuminances. Therefore, the values shown are the percentage that achieved the range defined between the minimum required illuminance of 300 lux and the maximum acceptable illuminance of 3000 lux. Figure 14b shows a temporal TSRE map of 374QS with the hourly values of kWh transmitted into the interior. In this manner, the optimal thermal efficiency of the PSS can be characterised for the whole year.

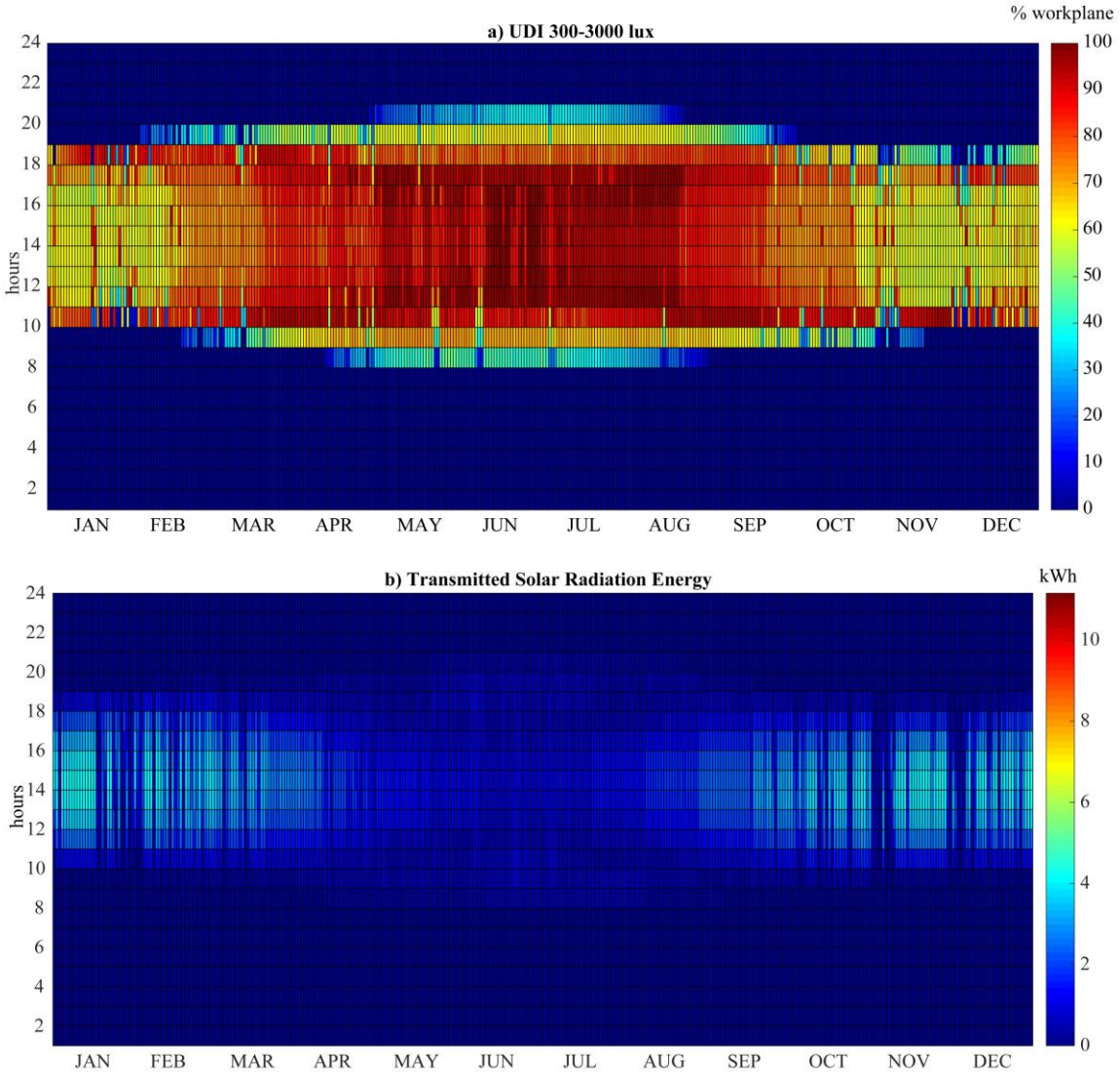

Figure 14. Temporal maps of 374QS.

Figure 15 shows the temporal illuminance and TSRE maps of the space with no PSS. Comparing Figure 14 with Figure 15 the differences between the use and non-use of PSS, in other words, the daylighting improvement throughout the year and the TSRE reduction which occurred mostly during

the winter months, can be observed.

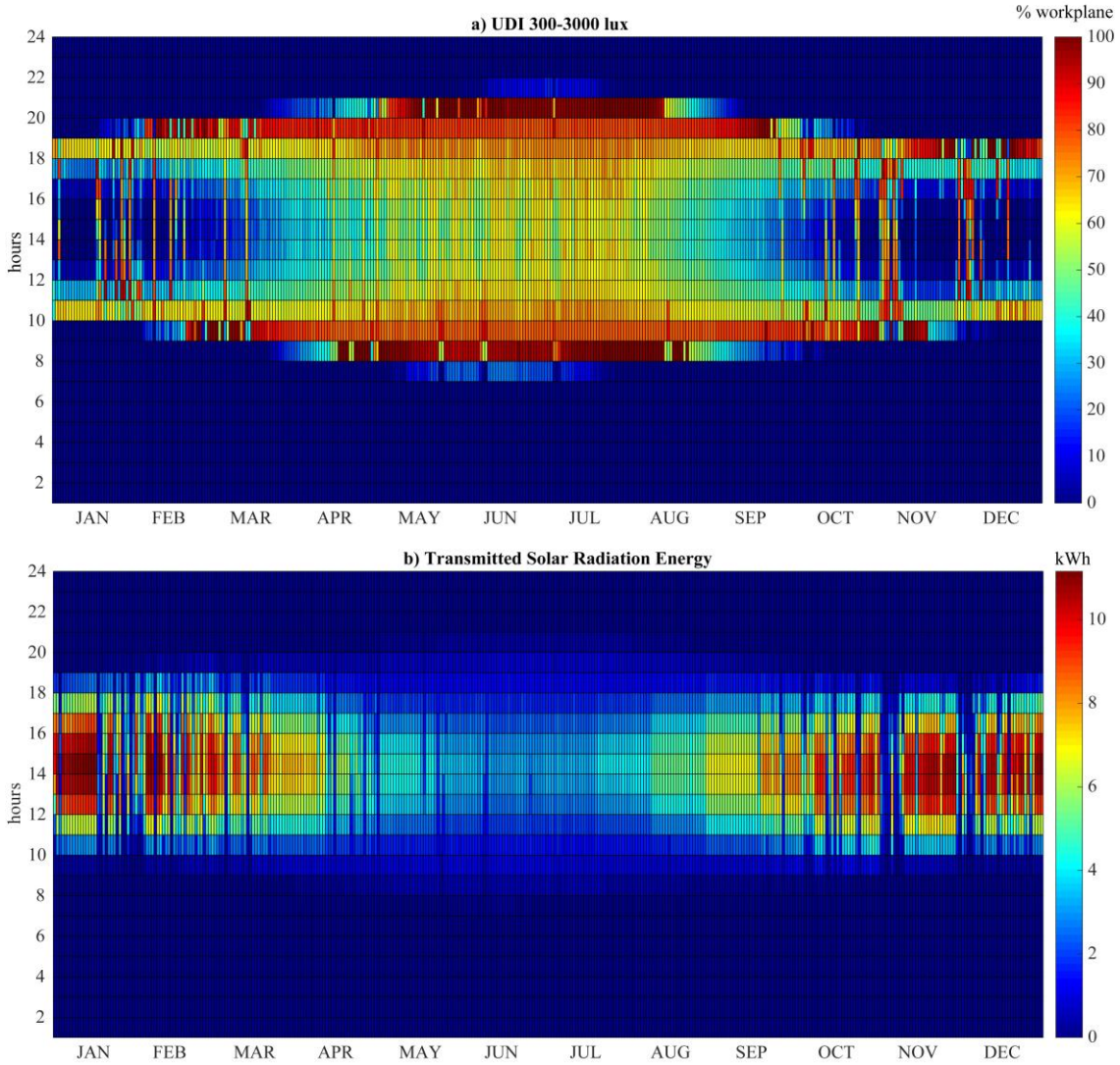

Figure 15. Temporal maps of REF100S.

4. Conclusions

This paper achieves the simultaneous study of two important PSS functions: those of providing adequate daylight in the workspace and preventing solar gains transmitted through the holes. Both aspects are translated into annual lighting, heating and cooling consumptions. Accordingly, this work presents a process of integrating a specific workflow for daylighting and energy analysis of complex geometries with the orthogonal method as a new tool for an adequate and novel comparative analysis of different typologies of PSS.

Firstly, the integrated workflow for evaluating and characterising PSS involves different daylight-thermal calculating software. DIVA is used for the daylighting calculation due to the precision of its calculation engine, RADIANCE, software widely validated in modelling daylight

illuminances and solar irradiations for complex geometries. Regarding the thermal performance, it follows a specific calculation process due to the drawbacks of the current energy program: the limit of digital construction for the PSS. Directly creating a complex surface geometry is infeasible using EnergyPlus. If a PSS is represented either by a surface with holes or by a mesh, it will be not recognized in the IDF file. In fact, calculations in EnergyPlus requires the representation of the geometries as single planes [20]. Hence, DIVA is used to calculate the hourly solar radiation falling on the façade with and without the PSS. The SC_{hourly} is then calculated and the use of Archism is integrated in order to determine an hourly transparency schedule which is assigned to simple surfaces in the thermal model in EnergyPlus, a validated simulation engine for performing energy calculations with simple geometries.

Secondly, it can be noticed that the workflow involves simulations in three main domains, namely daylight, solar irradiation and energy loads. Thus, the number of simulations increases and require quite a lot of time, being difficult to handle in practical situations and during the conceptual stages of building design. Therefore reducing the number of PSS configurations to be tested in order to optimise the design process is recommended. Using the DOA method, it is possible to obtain the greatest information from the results running the minimum number of computational simulations. DOA enables PSS design criteria in south-facing façades in Seville to be established: PP, without exceeding 37.5%, should be the leading factor in PPS design; M is second in importance and the use of larger-sized perforations is recommended, while S was statistically insignificant, giver greater design freedom.

PSS optimisation managed to find a balance between providing daylight and electricity consumption for lighting, heating and cooling. It was observed that, although all PSS managed to reduce solar gains due to irradiation, not all PSS gave sufficient levels of daylighting. In this sense, the use of indicators, such as the proposed index, enabled the integrated performance of the PSS's functions to be calculated and evaluated successfully.

With regard to the glazed façade, the optimised PSS increased the actual daylit area by 50% and reduced TSRE by 63%. Even though lighting consumption increased by 62%, this was compensated by a reduction of 58% and 86% in cooling and heating, respectively, thus achieving a 55% total annual saving in consumption. Moreover, the use of PSS on glazed façades is more effective than using a simple perforation, whose total annual consumption saving was 33%. It is therefore concluded that PSS use is effective on a southern orientation and that it should be implemented following the design criteria indicated.

Although this work applied the DOA method in order to optimise three design variables, it could also be used in future research simultaneously to take into account variables such as PSS thickness, materials and inclination. There are, furthermore, other functions which should be considered in PSS design, such as visual comfort (e.g. glare probability, uniformity of daylight illuminances) and the factor of exterior view. Future research can build upon this present one and explore these conditions.

Acknowledgements

The authors are grateful for the technical and financial support provided and wish to thank all involved for their invaluable collaboration.

Funding

This work was funded by the National Council of Science and Technology (CONACYT) of Mexico, under the Ph.D. scholarship of Doris A. Chi Pool; and the Institute of Architecture and Building Science (IUACC) of the University of Seville through members of the TEP-130 research group.

References

[1] O. Etman, O. Tolba, S. Ezzeldin, Double-Skin façades in Egypt between parametric and climatic approaches., in: Vol. 1 eCAADe: Conferences 1. (Ed.), Comput. Performance-Proceedings 31 St eCAADe Conf., Vol. 1 eCAADe: Conferences 1., Delft, The Netherlands: Deflt University of Technology, 2014: pp. 459–465.

[2] H. Poirazis, A. Blometerberg, M. Wall, Energy simulations for glazed office buildings in Sweden, Energy Build. 40 (2008) 1161–1170. doi:https://doi.org/10.1016/j.enbuild.2007.10.011.

[3] L. Bellia, F. De Falco, F. Minichiello, Effects of solar shading devices on energy requirements of standalone office buildings for Italian climates, Appl. Therm. Eng. 54 (2013) 190–201. doi:https://doi.org/10.1016/j.applthermaleng.2013.01.039.

[4] W. Wang, H. Rivard, R. Zmeureanu, Floor shape optimization for green building design, Adv. Eng. Informatics. 20 (2006) 363–378. doi:https://doi.org/10.1016/j.aei.2006.07.001.

[5] A. Villalba, J. Monteoliva, A. Pattini, Control solar sobre superficies vidriadas. Evaluación lumínica mediante métricas dinámicas y preferencia de usuarios a filtros solares., Av. En Energías Renov. Y Medio Ambient. 15 (2011) 79–88.

[6] E. Aljofi, The potentiality of reflected sunlight through Rawshan screens, in: Int. Conf. Passiv. Low Energy Cool. Built Environ., Heliotopos Conferences, Santorini, Greece, 2005: pp. 817–822.

[7] A. Pattini, A. Villalba, L. Córica, R. Rodríguez, L. Ferrón, Características ópticas de chapas metálicas perforadas de control solar en fachadas vidriadas., Av. En Energías Renov. Y Medio Ambient. 15 (2011) 123–132.

[8] A. De Gracia, A. Castel, L. Navarro, E. Oró, L.F. Cabeza, Numericall modelling of ventilated facades: A review, Renew Sustain Energy Rev. 22 (2013) 539–549. http://dx.doi.org/10.1016/j.rser.2013.02.029.

[9] C. Aparicio, J.L. Vivancos, P. Ferrer, R. Royo, Energy performance of a ventilated facade by simulation with experimental validation, Appl. Therm. Eng. 66 (2014). doi:10.1016/j.applthermaleng.2014.02.041.

[10] A. Sherif, A. El-Zafarany, R. Arafa, Improving the energy performance of desert buildings: the effect of using external perforated solar screens on the windo-to-wall ratio, in: Int. Symp. Sustain. Syst. Environ. ISSE'11, Sharjah, UAE, Sharjah, UAE, 2011.

[11] A. Sherif, A. Faggal, R. Arafa, External perforated solar screens for thermal control in desert environments: The effect of perforation percentage on energy loads., in: Renew. Energy 2010 Conf. Proceedings, Jt. with 4th Int. Sol. Energy Soc. Conf. Asia Pacific Reg., Yokohoma, Japan, Yokohoma, Japan, 2010.

[12] G.A. Mainini, T. Poli, M. Zinzi, A. Speroni, Spectral light transmission measure of metal screens for glass façades and assessment of their shading potential, Energy Procedia. 48 (2013) 1292–1301. doi:https://doi.org/10.1016/j.egypro.2014.02.146.

[13] G. Kim, Indoor and built predicted performance of shading devices for healthy visual environment, 2010.

[14] A. Sherif, H. Sabry, T. Rakha, External perforated solar screens for daylighting in residential desert buildings: Identification of minimum perforation percentages, Sol. Energy. 86 (2012) 1929–1940. doi:https://doi.org/10.1016/j.solener.2012.02.029.

[15] H. Sabry, A. Sherif, T. Rakha, M. Anees, Daylighting efficiency of external perforated solar screens: Effect of screen axial rotation under clear skies, in: Proc. Int. Conf. Sustain. Des. Constr., American Society of Civil Engineers,

Kansas City, Missouri, USA, 2011: pp. 283–291.
[16] E. Aljofi, Effect of the Rawshan on the provision of daylight for shopping precints, [Phd thesis] University of Wales, Cardiff, 1995.
[17] A. Sherif, H. Sabry, A. El-Zafarany, R. Arafa, T. Rakha, M. Anees, Balancing the energy savings and daylighting performance of external perforated solar screens, in: Proc. 27th Int. Conf. Passiv. Low Energy Archit. PLEA 2011 Archit. Sustain. Dev., Presses universitaires de Louvain, Louvain-la-Neuve, Belgium, 2011: pp. 807–812.
[18] A. Pino, W. Bustamante, F. Encinas, R. Escobar, Thermal and lighting behaviour of office buildings in Santiago of Chile, Energy Build. 47 (2012) 441–449. doi:https://doi.org/10.1016/j.enbuild.2011.12.016.
[19] G. Molina, W. Bustamante, J. Rao, P. Fazio, S. Vera, Evaluation of Radiance's genBSDF capability to assess bidirectional solar properties of complex fenestration systems, J. Build. Perform. Simul. 8 (2014) 216–225. doi:10.1080/19401493.2014.912355.
[20] DOE (U.S. Department of Energy), EnergyPlus Version 8.5 Documentation. Engineerging reference, LBNL (Lawrence Berkeley National Laboratory), California, 2016. doi:http://apps1.eere.energy.gov/buildings/energyplus/.
[21] D.W. Kim, C.S. Park, Difficulties and limitations in performance simulation of a double skin façade with EnergyPlus, Energy Build. 43 (2011) 3635–3645. doi:http://dx.doi.org/10.1016/j.enbuild.2011.09.038.
[22] G. Ramos, E. Ghisi, Analysis of daylight calculated using the EnergyPlus program, Renew Sustain Energy Rev. 14 (2010) 1948–1958. doi:https://doi.org/10.1016/j.rser.2010.03.040.
[23] A. Jakubiec, C.F. Reinhart, DIVA 2.0: Integrating daylight and thermal simulations using Rhinoceros 3D, Daysim and EnergyPlus, in: Proc. Build. Simul. 2011 12th Conf. Int. Build. Perform. Simul. Assoc., IBPSA (International Building Performance Simulation Association), Sydney, 2011: pp. 2202–2209.
[24] K. Lagios, J. Niemasz, C. Reinhart, Animated building performance simulation (abps)-linking rhinoceros/grasshopper with radiance/daysim, Proc. SimBuild. (2010). http://www.ibpsa.us/pub/simbuild2010/papers/SB10-DOC-TS06A-03-Lagios.pdf.
[25] O. Azadeh, Design optimization of a contemporary high performance shading screen – integration of "form" and simulation tools, in: Proc. Build. Simul. 2011 12th Conf. Int. Build. Perform. Simul. Assoc., IBPSA (International Building Performance Simulation Association), Sydney, 2011: pp. 2491–2498.
[26] J. González, F. Fiorito, Daylight design of office buildings: Optimisation of external solar shadings by using combined simulation methods, Buildings. 5 (2015) 560–580. doi:10.3390/buildings5020560.
[27] F. Trubiano, M.S. Roudsari, A. Ozkan, Building simulation and evolutionary optimization in the conceptual design of a high-performance office building, in: Proc. 13th Conf. Int. Build. Perform. Simul. Assoc., IBPSA, Chambery, France, 2013: pp. 1306–1314.
[28] G. Lobaccaro, F. Fiorito, G. Masera, D. Prasad, Urban solar district: A case study of geometric optimization of solar facades for a residential building in Milan, in: Proc. AuSES Sol. 2012 Conf., Melbourne, Australia, 2012.
[29] M. David, M. Donn, F. Garde, A. Lenoir, Assessment of the thermal and visual efficiency of solar shades, Build. Environ. 46 (2011) 1489–1496. doi:http://dx.doi.org/10.1016/j.buildenv.2011.01.022.
[30] G. Park, Analytic Methods for Design Practice, Springer London, Korea, 2007. doi:10.1007/978-1-84628-473-1.
[31] L. Franek, X. Jiang, Orthogonal design of experiments for parameter learning in image segmentation, Signal Processing. 93 (2013) 1694–1704. doi:http://dx.doi.org/10.1016/j.sigpro.2012.08.016.
[32] X. Gong, Y. Akashi, D. Sumiyoshi, Optimization of passive design measures for residential buildings in different Chinese areas, Build. Environ. 58 (2012) 46–57. doi:http://dx.doi.org/10.1016/j.buildenv.2012.06.014.
[33] H. Yi, R. Srinivasan, W. Braham, An integrated energy–emergy approach to building form optimization: Use of EnergyPlus, emergy analysis and Taguchi-regression method, Build. Environ. 84 (2015) 89–104. doi:https://doi.org/10.1016/j.buildenv.2014.10.013.
[34] L. Huang, J. Wu, Effects of the splayed window type on daylighting and solar shading, Build. Environ. 81 (2014) 436–447. doi:https://doi.org/10.1016/j.buildenv.2014.07.026.
[35] J. Wei, J. Zhao, Q. Chen, Optimal design for a dual-airflow window for different climate regions in China, Energy Build. 42 (2010) 2200–2205. doi:http://dx.doi.org/10.1016/j.enbuild.2010.07.016.
[36] D.A. Chi, D. Moreno, P. Esquivias, J. Navarro, Optimization method for perforated solar screen design to improve daylighting using orthogonal arrays and climate-based daylight modelling, J. Build. Perform. Simul. 10 (2016) 144–160. doi:10.1080/19401493.2016.1197969.

[37] The Society of Light and Lighting (SLL), The SLL Code for Lighting, CIBSE, London, UK, 2012.
[38] MITC (Ministerio de Industria Turismo y Comercio), Reglamento de instalaciones térmicas en los edificios, MITC, Madrid, España, 2013.
[39] G. Taguchi, T. Yokoyama, Taguchi methods: Design of experiments, ASI Press MI, Dearborn, 1993.
[40] J. Zhu, D. Chew, S. Lv, W. Wu, Optimization method for building envelope design to minimize carbon emissions of building operational energy consumption using orthogonal experimental design (OED), Habitat Int. 37 (2013) 148–154. doi:https://doi.org/10.1016/j.habitatint.2011.12.006.
[41] Minitab, MINITAB. User's Guide 2 : Data analysis and quality tools., Minitab Inc, State College, PA, USA, 2000.
[42] C.F. Reinhart, J. Wienold, DIVA for Grasshopper, (2011).
[43] S. Davidson, Grasshopper: Algorithmic Modelling for Rhino, (2013). http://www.grasshopper3d.com.
[44] G. Ward, The RADIANCE 4.2 Synthetic Imaging System, Univ. Calif. (1994) 1–7. http://radsite.lbl.gov/radiance/refer/ray.html#Materials (accessed January 15, 2015).
[45] C. Reinhart, O. Walkenhorst, Dynamic RADIANCE-based daylight simulations for a full-scale test office with outer venetian blinds., Energy Build. 33 (2001) 683–697. doi:10.1016/S0378-7788(01)00058-5.
[46] C. Reinhart, P. Breton, Experimental Validation Of 3ds Max® Design 2009 And Daysim 3.0, Leukos. 6 (2009) 7–35. doi:10.1582/LEUKOS.2009.06.01001.
[47] G. Ward, Measuring and modeling anisotropic reflection, Comput. Graph. (ACM). 26 (1992) 265–272.
[48] C. Reinhart, M. Andersen, Development and validation of a radiance model for a translucent panel, Energy Build. 38 (2006) 890–894. doi:https://doi.org/10.1016/j.enbuild.2006.03.006.
[49] A. Tsangrassouis, V. Bourdakis, Comparison of radiosity and ray-tracing techniques with a practical design procedure for the prediction of daylight levels in atria, Renew. Energy. 28 (2003) 2157–2162. doi:https://doi.org/10.1016/S0960-1481(03)00078-8.
[50] C. Reinhart, T. Rakha, D. Weissman, Predicting the Daylit Area — A Comparison of Students Assessments and Simulations at Eleven Schools of Architecture, Leukos. 10 (2014) 193–206. doi:10.1080/15502724.2014.929007.
[51] J. Mardaljevic, M. Andersen, N. Roy, J. Christoffersen, Daylighting metrics: Is there a relation between Useful Daylight Illuminance and Daylight Glare Probability?, in: Proc. Build. Simul. Optim. Conf. BSO12, IBPSA, Loughborough, UK, 2012: pp. 189–196.
[52] C. Reinhart, J. Wienold, The daylighting dashboard - A simulation-based design analysis for daylit spaces, Build. Environ. 46 (2011) 386–396. doi:https://doi.org/10.1016/j.buildenv.2010.08.001.
[53] J. Mardaljevic, A. Nabil, The useful daylight illuminance paradigm : A replacement for daylight factors, in: Lux Eur., Ludwig Erhard Haus Industrie- und Handelskammer zu Berlin, Berlin, 2005: pp. 169–174.
[54] A. Nabil, J. Mardaljevic, Useful daylight illuminance: A new paradigm for assessing daylight in buildings, Light. Res. Technol. 37 (2005) 41–59. doi:10.1191/1365782805li128oa.
[55] IESNA (Illuminating Engineering Society of North America), Daylight Metrics Comitte, Approved method: IES Spatial Daylight Autonomy (sDA) and Annual Sunlight Exposure (ASE), IESNA, New York, 2013.
[56] ASHRAE (American Society of Heating Refrigerating and Air-Conditining Engineers), ASHRE/IESNA Standard 90.1-2016. Energy standard for buildigns except low-rise residendial buildings, Atlanta, 2016.
[57] C. Reinhart, Lightswitch-2002: A model for manual and automated control of electring lighting and blinds., Sol. Energy. 77 (2004) 15–28. doi:https://doi.org/10.1016/j.solener.2004.04.003.
[58] IESNA (Illuminating Engineering Society of North America), Lighting handbook 10th Edition, IESNA Publications Department, New York, 2011.
[59] R. McNeel, Associates, Rhinoceros Version 4.0, (2010).
[60] T. Dogan, Archsim Primer. An introduction to energy modeling with Grasshopper, GitBook, 2016. https://tkdogan.gitbooks.io/archsim-primer/content/index.html.
[61] F. Garde, M. David, L. Adelard, E. Ottenwelter, Elaboration of thermal standards for French tropical islands: presentation of the PERENE project, in: Proc. Clima 2005, Lausanne, Switzerland, 2005.
[62] R. McNeel, Rhinoceros: Nurbs Modeling for Rhino (Versión 4.0 SR 8), (2010). www.rhino3d.com.
[63] J. Yang, H. Fu, M. Qin, Evaluation of Different Thermal Models in EnergyPlus for Calculating Moisture Effects on Building Energy Consumption in Different Climate Conditions, Procedia Eng. 121 (2015) 1635–1641. doi:https://doi.org/10.1016/j.proeng.2015.09.194.
[64] ASHRAE (American Society of Heating Refrigerating and Air-Conditining Engineers), ASHRAE Handbook -

Fundamentals, I-P Editio, ASHRAE, Inc, Atlanta, 2013.
[65] J. Mardaljevic, Spatio-temporal dynamics of solar shading for a parametrically defined roof system, Energy Build. 36 (2004) 815–823.

View publication stats